MARTIN MARIETTA ENERGY SYSTEMS LIBRARIES
3 4456 0050177 6

ornl

OAK
RIDGE
NATIONAL
LABORATORY

UNION
CARBIDE

NUREG/CR-3181
(ORNL/TM-8683)

Quantity and Nature of LWR Aerosols Produced in the Pressure Vessel During Core Heatup Accidents-A Chemical Equilibrium Estimate

R. P. Wichner
R. D. Spence

Prepared for the
U.S. Nuclear Regulatory Commission
Office of Nuclear Regulatory Research
Under Interagency Agreement DOE 40-551-75

OAK RIDGE NATIONAL LABORATORY
CENTRAL RESEARCH LIBRARY
CIRCULATION SECTION
4500N ROOM 175
LIBRARY LOAN COPY
DO NOT TRANSFER TO ANOTHER PERSON
If you wish someone else to see this report, send in name with report and the library will arrange a loan.
UCN-7969 (3 9-77)

OPERATED BY
UNION CARBIDE CORPORATION
FOR THE UNITED STATES
DEPARTMENT OF ENERGY

Printed in the United States of America. Available from
National Technical Information Service
U.S. Department of Commerce
5285 Port Royal Road, Springfield, Virginia 22161

Available from
GPO Sales Program
Division of Technical Information and Document Control
U.S. Nuclear Regulatory Commission
Washington, D.C. 20555

This report was prepared as an account of work sponsored by an agency of the United States Government. Neither the United States Government nor any agency thereof, nor any of their employees, makes any warranty, express or implied, or assumes any legal liability or responsibility for the accuracy, completeness, or usefulness of any information, apparatus, product, or process disclosed, or represents that its use would not infringe privately owned rights. Reference herein to any specific commercial product, process, or service by trade name, trademark, manufacturer, or otherwise, does not necessarily constitute or imply its endorsement, recommendation, or favoring by the United States Government or any agency thereof. The views and opinions of authors expressed herein do not necessarily state or reflect those of the United States Government or any agency thereof.

NUREG/CR-3181
ORNL/TM-8683
Dist. Category R3

Chemical Technology Division

QUANTITY AND NATURE OF LWR AEROSOLS PRODUCED IN THE PRESSURE VESSEL DURING CORE HEATUP ACCIDENTS — A CHEMICAL EQUILIBRIUM ESTIMATE

R. P. Wichner
R. D. Spence

Manuscript Completed — September 1983
Date Issued — March 1984

NOTICE This document contains information of a preliminary nature. It is subject to revision or correction and therefore does not represent a final report.

Prepared for the
U.S. Nuclear Regulatory Commission
Office of Nuclear Regulatory Research
Washington, D.C. 20555
under Interagency Agreement DOE 40-551-75

NRC FIN No. B0127

Prepared by the
OAK RIDGE NATIONAL LABORATORY
Oak Ridge, Tennessee 37831
operated by
UNION CARBIDE CORPORATION
for the
U.S. DEPARTMENT OF ENERGY
under Contract No. W-7402-eng-26

MARTIN MARIETTA ENERGY SYSTEMS LIBRARIES
3 4456 0050177 6

ABSTRACT

The degree of vaporization of LWR core materials was estimated using a highly idealized procedure involving (1) specification of the phases that are present for both structural and fuel material; (2) estimation of the vapor pressures exerted by the individual components of each phase; and (3) assuming a degree of vaporization of each phase constituent, to allow equilibration between gaseous and condensed species within the assumed pressure vessel volume. Obviously, the degree of vaporization of many core materials is limited by other complex factors such as local mass transport conditions and solid-phase diffusion rates; however, the results obtained in this study serve to illustrate the types of driving forces for vaporization that are present and to give some indication of the composition of the vaporized material. Some comparisons are provided with estimated degrees of core vaporization from other sources.

In addition to estimated degrees of vaporization, information is included regarding the projected chemical forms of the condensed material for the expected range of oxygen potentials in the reactor vessel.

CONTENTS

	Page
ABSTRACT	iii
LIST OF FIGURES	vii
LIST OF TABLES	viii
1. INTRODUCTION	1
2. AEROSOL FORMATION MECHANISMS	2
3. ESTIMATED QUANTITIES AND COMPOSITION OF AEROSOLS	3
3.1 VAPOR PRESSURES OF STRUCTURAL AND CONTROL ROD MATERIALS	4
3.2 VAPOR PRESSURES OF FUEL MATERIALS	9
3.3 VOLATILITIES OF ALKALINE EARTH SPECIES	10
3.4 DEGREE OF VAPORIZATION OF CORE MATERIAL	14
3.5 EFFECT OF BORON SOURCES ON COMPOSITION OF THE AEROSOLS	17
3.6 COMPARISON WITH OTHER ESTIMATES	21
4. OXYGEN POTENTIALS IN THE REACTOR VESSEL	24
5. CHEMICAL FORMS OF REACTOR VESSEL AEROSOLS	26
6. SUMMARY AND CONCLUSIONS	29
7. REFERENCES	31

LIST OF FIGURES

Figure		Page
1.	Volatility of lanthanum oxide due to the reaction $2\langle La_2O_3\rangle = 4(LaO) + (O_2)$	11
2.	Volatility of cerium oxide due to the reaction $2\langle Ce_2O_3\rangle = 4(CeO) + (O_2)$	12
3.	Equilibrium pressure of $Ba(OH)_2$ from the reaction $\langle BaO\rangle + (H_2O) = (Ba(OH)_2)$ and vapor pressure of $Ba(OH)_2$ above the liquid	13
4.	Estimated H_2/H_2O ratios in the reactor vessel from time of initial cladding failure	25
5.	Chemical forms of structural aerosols	28

LIST OF TABLES

Table		Page
1.	Amounts and properties of structural and control rod materials in a PWR core	5
2.	Amounts and properties of structural material in a BWR core	6
3.	Amounts and properties of fuel and fission products in a core	7
4.	Examples of activity coefficients in binary alloys at 773 K	9
5.	Estimated vaporized fractions for PWR cores with and without silver alloy control rods	15
6.	Estimated vaporized fractions for BWR cores	16
7.	Amounts and properties of boron sources in a PWR core	18
8.	Amounts and properties of boron sources in a BWR core	20
9.	Estimated vaporized fractions for PWR cores with and without silver alloy control rods containing boron	22
10.	Estimated vaporized fractions for BWR cores containing boron	23
11.	Predicted amounts of structural aerosol formed under core-melt conditions	26
12.	Chemical forms of aerosols in pressure vessel prior to failure	30

QUANTITY AND NATURE OF LWR AEROSOLS PRODUCED IN THE PRESSURE VESSEL DURING CORE HEATUP ACCIDENTS — A CHEMICAL EQUILIBRIUM ESTIMATE

R. P. Wichner
R. D. Spence

1. INTRODUCTION

The transport of fission products on, or in the form of, aerosols is recognized as a principal mode of movement from the source of their production (the failed fuel element) through the various components of a nuclear power reactor. Fission products may either condense as aerosol particles or deposit onto existing particles of some other material by processes such as condensation, chemisorption, or chemical reaction. It is therefore important to know the quantity and the nature of aerosols produced by an overheated reactor core. The best way to accomplish this is to use experimentally determined vaporization rates adapted to the projected core overheat conditions, as was done in two recent studies.[1,2] Unfortunately, this method alone does not develop the understanding required to confidently extend experimental data to the various projected accident environments.

This report provides an estimate of the quantity of aerosol produced by an overheated LWR core in the pressure vessel prior to melt-through and an evaluation of the subsequent chemical form of the vaporized material. Although this study was done by using highly idealized assumptions, it was felt that the results would aid in the recognition of aerosol formation processes and consequently would be helpful in determining the appropriateness of planned experimental work.

It was assumed in this case that the entire core generated vapor at a uniform constant temperature, 2700 K, roughly the expected melting point of the fuel/structure mixture. Although this temperature is above the melting point of the pressure vessel, the molten mix and the associated vapors are assumed to be contained within the volume of the pressure vessel. The degree of vaporization of each component is governed by several factors. First of all, one needs to know the chemical form of the vaporizing species. In many important cases, however, the material vaporizes from a surrounding host phase which can profoundly affect the inherent volatility. Therefore, the phases that exist (or are formed under core-melt conditions) need to be identified, not only because of the normally expected reduction in vapor pressure due to dilution, but also because intermolecular forces within the phase may further affect volatility. Cursory examination of a standard reference document[3] indicates that intermolecular forces within a phase may cause deviations from Raoult's law by factors of $\sim 10^{-5}$ to $\sim 10^{2}$. Nevertheless, the estimates of aerosol composition in this report are based on Raoult's law and thus could be in considerable error.

It should also be kept in mind that vaporization under these extreme conditions is frequently not the simple process of generating a "molecular

fleeing tendency" in a condensed phase, as is common at lower temperatures. Since high-temperature vaporization is frequently accompanied by chemical reaction, volatility is not a unique function of temperature but also depends very strongly on the chemical environment (principally the oxygen potential). This will be seen to be true for the rare earth oxides and probably applies to all refractory oxides as well.

In this study six phases were assumed to exist in the overheated core, four consisting of structural/control rod materials and two consisting of fuel. A static system bounded by the pressure vessel volume was also assumed, with vaporization inhibited only by the developed partial pressure of the material. For some highly volatile materials, such as elemental cesium, iodine, and tellurium, vaporization is complete under the assumed conditions and the developed partial pressures in these cases depend on their available masses rather than their vapor pressures. Following vaporization, the material will condense into either an elemental or an oxidic form, depending primarily on the oxygen potential in the gas space of the pressure vessel. The elements projected to exist as oxides or primarily as metals are given in Sect. , based on an assumed range of oxygen potentials.

The degree of vaporization of the core estimated by these idealized assumptions was then compared with estimates or assumptions used in other studies. Despite the acknowledged idealizations, agreement with the results of other studies is fairly good.

2. AEROSOL FORMATION MECHANISMS

The primary mechanism for the formation of aerosols in the reactor vessel is that of vaporization of materials from an overheated core followed by condensation as the materials are convected to lower-temperature zones. Some fairly complex and, as yet, not well understood phenomena are involved in this mechanims. For example, the condensation process may be directed toward either the formation of primary aerosol nuclei or the deposition on existing surfaces. Since homogeneous nucleation generally involves large supersaturation ratios, such as those required for the formation of new surfaces, it appears more likely that the bulk of the aerosol mass results from condensation onto existing nuclei formed from materials likely to condense first (e.g., the aerosol materials with lowest volatilities). Consequently, determination of the actual mass of aerosol formed requires an appreciation of the competition between solid surfaces and aerosol particles for the condensing material.

The relative rates of condensation onto existing aerosol and adjacent wall surfaces can depend on both the relative mass transfer rates to these geometries and the relative value of the thermodynamic driving force. Since the aerosol surface may be expected to be at the temperature of the gas in which it is carried (which is usually much hotter than adjacent structural surfaces, at least during the early, heatup phase of a severe accident sequence) the driving force for condensation onto structural surfaces would greatly exceed that for condensation onto

aerosol particles. On the other hand, mass transfer coefficients for small particles generally exceed those estimated for larger structures. Roughly speaking, mass transfer coefficients for ~1-μm spherical particles are of the order of 100 cm/s, compared with 0.1 to 1 cm/s for structural surfaces, which may tend to compensate for the comparatively lower driving force for condensation. A proper assessment of the mass of aerosol produced therefore requires an estimation of the relative rates of condensation of vaporized material between suspended nuclei and wall structure. This relative rate estimate, in turn, will depend on estimation of the aerosol nucleation rate as well as on specification of local flows and temperatures which affect mass transfer rates.

Any chemical reaction effects that may occur must be superimposed onto the above considerations. The thermodynamically favored aerosol chemical forms under projected reactor vessel conditions are discussed in Sect. 5. In some cases (notably zirconium), the thermodynamically stable aerosol form differs from the bulk material present; that is, the stable form must be the oxide under any expected temperature or oxygen potential, whereas the metal is what is initially present. In view of the much higher volatility of the metal, it is reasonable to assume that the predominant vaporizing form is the metal, which would then be expected to react in the steam/H_2 environment to form ZrO_2. Thus we would expect the mass of zirconium aerosol formed to be related to zirconium volatility, but nucleation or condensation behavior to be more of a function of the properties of the oxide. As shown in Sect. 5, vaporization of iron, indium (from the control rod alloy), and molybdenum could also fall into the same category with zirconium, at least for the highest range of expected oxygen potentials.

In addition, it should be noted that chemical reaction sometimes accompanies the vaporization process, resulting in unexpectedly high volatility. This appears to be a fairly common phenomenon for high-temperature vaporizations of refractory oxides (e.g., La_2O_3, CeO_2, and SiO_2). Section 3 shows that, in a reducing atmosphere, rare-earth oxides vaporize as the monoxide with a significantly higher effective volatility than expected from an examination of condensed phase properties alone.

3. ESTIMATED QUANTITIES AND COMPOSITIONS OF AEROSOLS

A highly idealized method was used to predict the elemental composition and amount of aerosols produced in the pressure vessel by an overheated LWR core. For simplicity, the main assumption was that of a static system with an enclosed boundary formed by the primary system. Into this enclosure (the pressure vessel), core structure and fuel material evaporate in proportion to the best estimates of the vapor pressures of the evaporating species. Vaporization is complete for highly volatile materials (e.g., cesium), and the resulting partial pressure depends on the quantity of material present, the volume

into which it vaporizes, and the temperature. Less volatile materials are assumed to vaporize until a vapor-solid or vapor-liquid equilibrium is achieved.

It is recognized that such assumptions represent a highly idealized version of the actual situation. Nevertheless, this is a useful learning exercise which helps us develop an understanding of the important phenomena involved in aerosol generation.

This exercise was carried out for a typical PWR core, with and without silver control rods, and for a typical BWR core. Table 1 lists the masses of structural and control rod material found in a typical PWR, as given in ref. 4. Table 2 lists the masses of structure found in a typical BWR.

3.1 VAPOR PRESSURES OF STRUCTURAL AND CONTROL ROD MATERIALS

It seems reasonable to assume that the dominant vaporizing species for structural and control rod materials is the metal, even though the oxide may be the most thermodynamically stable form in some cases (e.g., zirconium and chromium). An oxide crust will undoubtedly be present on the Zircaloy and stainless steel; however, the base metal, which has the higher vapor pressure, is still likely to be the major vaporizing form.

The vapor pressure of each pure structural/control rod material in a PWR core at 2700 K, which is approximately the melting point of the core mixture, is given in Table 1. The "effective vapor pressure," which is also included, is assumed to be that calculated using Raoult's law for the phase containing the element in question.

Identification of the phases present during core melting is a necessary prerequisite to the determination of vaporization rates. In the present study, we assumed the existence of the following phases:

Structural and control rod materials (see Tables 1 and 2)	Fuel material (see Table 3)
Zircaloy-4	UO_2-rich phase
Stainless steel	Noble metals
Control rod alloy	
Inconel X	

Although this represents a gross simplification of the actual situation, it can serve as the basis for a preliminary study. Actually, other phases will form upon core heatup, and the rate and extent of phase formation are crucial for proper determination of volatilities. A very significant case may be Ag-Zr alloy formation, which strongly influences (probably diminishes) silver volatility.

Table. 1. Amounts and properties of structural and control rod materials in a PWR core

Constituent	Amount (kg)	Amount (mol)	Mol fraction in phase[a]	Evaporating material: Form	Melting point (°C)	Boiling point (°C)	Temperature = 2700 K (2427°C): Vapor pressure (bar)	Effective vapor pressure[b] (bar)	Maximum pressure[c] (bar)
				Zircaloy-4					
Zr	16,200	1.78×10^5	0.98	Metal	1852	4375	1.9×10^{-5}	1.9×10^{-5}	71.0
Sn	240	2.02×10^3	0.011	Metal	232	2687	0.41	4.5×10^{-3}	0.8
Fe	35	6.27×10^2	3.4×10^{-3}	Metal	1535	2862	0.054	1.9×10^{-4}	0.25
Total	16,500	1.80×10^5							
				Stainless steel[d]					
Fe	1,360	2.44×10^4	0.67	Metal	1535	2862	0.054	0.036	9.7
Cr	380	7.31×10^3	0.20	Metal	1903	2642	0.34	0.068	2.9
Ni	200	3.41×10^3	0.093	Metal	1453	2914	0.014	1.3×10^{-3}	1.4
Mn	40	7.28×10^2	0.020	Metal	1244	2040	4.16	0.083	0.29
Si	20	7.12×10^2	0.019	Metal	1412	3267	0.017	3.2×10^{-4}	0.29
Total	2,010	3.67×10^4							
				Control rods					
Ag	2,260	2.10×10^4	0.81	Metal	961	2210	2.42	2.0	8.4
In	425	3.70×10^3	0.14	Metal	156	2000	5.1	0.71	1.5
Cd	142	1.26×10^3	0.049	Metal	321	765	867	42.5	0.50
Total	2,830	2.59×10^4							

[a]Assumed phases: Zircaloy-4, stainless steel, and control rod alloy.

[b]Assuming Raoult's law in phase.

[c]Pressure exerted if completely vaporized within confines of pressure vessel, all at 2700 K. The lesser of the two — effective vapor pressure and maximum pressure — was used as the elemental vapor pressure from each phase.

[d]Includes only core stainless steel (not internal steel, vessel bottom, and liner, which would add another 270,000 kg). Since the relative composition would not change, the effective vapor pressure would not change; only the maximum pressure and percent vaporized would show a variation. This extra mass of steel would tend to cause dilution in a molten mix of phases but would have no effect here because separate phases are assumed for these calculations.

Table 2. Amounts and properties of structural material in a BWR core

Constituent	Amount (kg)	Amount (mol)	Mol fraction in phase[a]	Evaporating material: Form	Melting point (°C)	Boiling point (°C)	Temperature = 2700 K (2427°C): Vapor pressure (bar)	Effective vapor pressure (bar)	Maximum pressure[b] (bar)
				Zircaloy-4					
Zr	59,300	6.50×10^5	0.98	Metal	1852	4375	1.9×10^{-5}	1.9×10^{-5}	260
Sn	875	7.37×10^3	0.011	Metal	232	2687	0.41	0.0045	3.0
Fe	35	6.27×10^2	3.4×10^{-3}	Metal	1535	2862	0.054	1.8×10^{-4}	0.9
Total	60,400	6.16×10^5							
				Stainless steel[c]					
Fe	7,700	1.38×10^5	0.66	Metal	1535	2862	0.054	0.036	55.2
Cr	2,160	4.15×10^4	0.20	Metal	1903	2642	0.33	0.068	17.0
Ni	1,140	1.93×10^4	0.093	Metal	1453	2914	0.075	0.007	7.7
Mn	230	4.13×10^3	0.020	Metal	1244	2040	4.16	0.083	1.7
Si	110	4.06×10^3	0.020	Metal	1412	3267	0.017	3.2×10^{-4}	1.6
Total	11,350	2.08×10^5							
				Inconel X					
Ni	15,300	2.10×10^5	0.70	Metal	1953	2914	0.075	0.053	104
Cr	3,160	6.07×10^4	0.16	Metal	1903	2642	0.33	0.053	24.0
Fe	1,470	2.64×10^4	0.071	Metal	1535	2862	0.054	0.0038	11.0
Ti	530	1.10×10^4	0.029	Metal	1668	3260	0.010	2.9×10^{-4}	4.4
Al	190	6.93×10^3	0.019	Metal	660	2450	0.87	0.017	2.8
Mn	150	2.68×10^3	0.0072	Metal	1244	2040	4.16	0.030	1.1
Si	60	2.24×10^3	0.0060	Metal	1412	3267	0.017	1.0×10^{-4}	0.9
Total	21,000	3.73×10^5							

[a] Assumed phases: Zircaloy-4, stainless steel, and Inconel X.

[b] Pressure exerted if completely vaporized within confines of pressure vessel, all at 2700 K. Either the effective vapor pressure or the maximum pressure — whichever was the lesser — was used as the elemental vapor pressure from each phase.

[c] Includes only core stainless steel (not internal steel and vessel bottom, which would add another 304,000 kg). Since the relative composition would not change, the effective vapor pressure also would not change; only the maximum pressure and the percent vaporized would show variation. This extra mass of steel could cause dilution in a molten mix of phases; however, it would have no effect here because separate phases are assumed for these calculations.

Table 3. Amounts and properties of fuel and fission products in a core[a]

Constituent	Amount: PWR (mol)	Amount: BWR (mol)	Amount: Mol fraction in phase[b]	Evaporating material: Form	Evaporating material: Melting point (°C)	Evaporating material: Boiling point (°C)	Temperature = 2700 K (2427°C): Vapor pressure (bar)	Temperature = 2700 K (2427°C): Effective vapor pressure[c] (bar)	Temperature = 2700 K (2427°C): Maximum pressure[d] (bar): PWR	Temperature = 2700 K (2427°C): Maximum pressure[d] (bar): BWR
Semivolatiles										
I, Br	146	308		I_2	114	183	High	*e*	0.059	0.12
Cs, Rb	1624	3222		Cs	29	700	High	*e*	0.65	1.4
Te	253	533		Te	450	998	High	*e*	0.10	0.21
Oxide fuel matrix										
U	2.95×10^5	6.22×10^5	0.97	UO_2	2830		0.002	0.002	118	249
Ba, Sr	1279	2696	0.0042	BaO	1920	(2750)	3.2	0.014	0.51	1.08
Rare earths	4471	9421	0.015	La_2O_3	2320		0.06	1×10^{-3}	1.78	3.74
Zr, Nb	2402	5060	0.0089	ZrO_2	2720	(4300)	Low	Low	1.09	2.29
Noble metal inclusions										
Mo	2179	4591	0.39	Metal	2610	5560	5.3×10^{-6}	2.1×10^{-6}	0.87	1.8
Ru	1527	3323	0.28	Metal	2500	4900	2.3×10^{-5}	6.4×10^{-6}	0.63	1.3
Pd	914	1927	0.16	Metal	1552	3980	0.076	0.012	0.37	0.77
Tc	518	1091	0.095	Metal	2200		1×10^{-4}	9.5×10^{-6}	0.21	0.44
Rh	296	624	0.053	Metal	1966	4500	5.3×10^{-4}	2.8×10^{-5}	0.12	0.25
Ag	58	122	0.010	Metal	961	2210	2.42	0.024	0.023	0.049

[a] Quantities of fission products are based on an ORIGEN calculation for the Browns Ferry BWR at essentially infinite time at initial unloading. The differences between a PWR and a BWR are simply the differences in core fuel mass.

[b] In assumed phases: phase 1 (UO_2-La_2O_3-BaO-ZrO_2); phase 2 (noble metals).

[c] Vapor pressure times mol fraction in phase.

[d] Pressure exerted if completely vaporized within confines of pressure vessel, all at 2700 K. A volume of 548 m^3 (BWR) was used for both PWR and BWR calculations even though the PWR will have a smaller volume.

[e] Completely vaporized.

The greatest possible effect of solution formation would be vapor-pressure reduction of the more volatile core constituents. The above-mentioned solubility of silver in zirconium is perhaps the most prominent example. Other possibilities that may significantly affect aerosol formation are alloy formations involving Cs (perhaps with Sn), Te, Cd, In, and Sn, which together with silver comprise the most volatile metal group. Only sparse data are available on the possible alloying effects involving these volatile metals.

Vapor-pressure reduction by alloy formation would be caused by two mechanisms: (1) dilution and (2) interatomic forces between the solute and the host material.

The effect of dilution can be seen directly from Raoult's law:

$$P^*_{Ag} = N_{Ag}\ P^*_{Ag,o}\ , \tag{1}$$

where

P^*_{Ag} = vapor pressure of silver above solution at the given temperature,

N_{Ag} = mol fraction of silver in the solution,

$P^*_{Ag,o}$ = vapor pressure of pure silver at the given temperature.

Raoult's law does not normally apply to dilute solutions, however, and significant deviations may occur at mol fractions below ~0.85. Most deviations appear to be negative (i.e., $P^* < NP^*_o$) and can be as great as a factor of 10^{-5}. Deviations from Raoult's law are expressed by adding an activity coefficient, γ, to Eq. (1), as follows:

$$P^*_{Ag} = \gamma\ N_{Ag}\ P^*_{Ag,o}\ . \tag{2}$$

Negative deviations from Raoult's law (i.e., γ values of <1) are caused by chemical affinity of the host material for the solute. An example is seen in the Na-Sn system (Table 4), where a vapor-pressure reduction (below that predicted by Raoult's law) of $\sim 5 \times 10^{-3}$ at low sodium concentrations is evident.[3] Therefore, one may suspect that cesium may similarly be sequestered by tin, if the opportunity arises.

The Ag-In system is an example of an ideal solution ($\gamma = \sim 1$), while the Fe-Zn alloy shows a case where the deviation is positive (i.e., zinc vapor pressures exceed Raoult's law predictions).[3]

Cursory examination of a standard reference[4] indicates that activity coefficients may range between $\sim 10^{-6}$ (e.g., for the Al-Ni system) and ~500 (e.g., in the Ag-Mn system). This represents the maximum range of error that is possible by blindly applying Raoult's law to alloy systems.

Table 4. Examples of activity coefficients in binary alloys at 773 K

Alloy system	Mol fraction of first alloy composition	Activity coefficient, γ, of first alloy composition
Na-Sn	0.1	0.005
	0.2	0.007
	0.3	0.015
Ag-In	0.2	1.04
	0.4	1.07
	0.6	0.94
Zn-Fe	0.1	3.6
	0.2	2.5
	0.3	1.8

Source: R. Hultgren et al., Selected Values of the Thermodynamic Properties of Binary Alloys, American Society of Metals, Metals Park, Ohio, 1973.

Column 8 in Tables 1 and 2 lists the vapor pressure of each pure structural/control rod material at 2700 K, approximately the melting point of the core mixture. Column 9 gives the effective vapor pressure, assuming dilution only (i.e., Raoult's law) in the phase indicated. In the case of cadmium, the effective vapor pressure is sufficiently high that all the assumed 142 kg of metal in the core becomes gaseous at 2700 K (assuming a pressure vessel volume of 548 m^3 at 2700 K). The partial pressure of cadmium is thus limited by the quantity of material and does not reach that predicted by its vapor pressure.

3.2 VAPOR PRESSURES OF FUEL MATERIALS

Table 3 lists the quantities of fuel and fission product material in a typical equilibrium core corresponding to the amounts of structural material given in Tables 1 and 2.

Only two fuel phases are assumed here: (1) an oxidic phase containing the alkaline-earth and rare-earth oxides, as well as ZrO_2 and Nb_2O_3, in the UO_2 host; and (2) a metallic phase containing the noble metals.

The precise vaporizing forms of the halogens, cesium and tellurium are not required to be known, since each possible form has a sufficiently high vapor pressure at 2700 K to completely vaporize these materials into

the pressure vessel volume. For example, the extrapolation of results reported by Besmann and Lindemer[5] and Lindemer et al[6] (although their data for the cesium/UO_2 system were obtained at ≤1400 K) to 2700 K indicates that the stable cesium species in UO_2 would be cesium metal with an extremely high vapor pressure. Should this ultimately prove to be incorrect and a cesium uranate is actually shown to be the stable form, it would not matter since the vapor pressure of cesium over cesium uranate is sufficiently high at these temperatures to completely vaporize cesium.

Perhaps it is important to point out the unexpectedly high vapor pressures exerted by the rare-earth oxides at the oxygen potentials typical of irradiated fuel (i.e., (~ -400 kJ/mol). This was apparently first reported by Pearson and Lindemer,[7,8] who concluded that rare-earth oxides dissociate to a variety of forms to some degree at high temperatures and low oxygen levels. The strongest tendency results in the formation of the gaseous monoxide:

$$2\langle La_2O_3\rangle = 4(LaO) + (O_2) \quad , \qquad (3)$$

where < > signifies the solid and ( ) denotes the gaseous form. At low oxygen pressure, Eq. (3) is driven to the right so that the vapor pressure exerted by LaO over La_2O_3 is surprisingly high for such a refractory material. Revised Ellingham diagrams for monoxide formation over La_2O_3 and Ce_2O_3 are shown in Figs. 1 and 2, which are taken from refs. 7 and 8, respectively.

It may be deduced from Fig. 1 that the LaO pressure over pure La_2O_3 at a temperature of 2700 K and an oxygen potential of -418 kJ/mol (-100 kcal/mol), which is typical for irradiated UO_2, is ~0.06 bar. An approximately similar vapor pressure is indicated for CeO in Fig. 2 for the same conditions except that the solid phase consists of a solution of CeO_{2-x}, where x varies from 0 to 0.5. Thus, a vapor pressure of ~0.06 bar was assumed for the rare-earth oxides as a group. Since the total mol fraction for rare earths in UO_2 irradiated to 27 MWd/kg is ~0.015, the effective vapor pressure of the lanthanum group above UO_2 was estimated as $(0.06 \times 0.015 = 0.0009) \sim 1 \times 10^{-3}$ bar (Table 3).

3.3 VOLATILITIES OF ALKALINE-EARTH SPECIES

In view of the high oxygen acquisitiveness of the alkaline-earth elements barium and strontium, the oxides of these elements undoubtedly form quickly upon release from fuel. In the presence of steam, however, the more volatile hydroxides tend to form via reaction with H_2O,

$$\langle BaO\rangle + (H_2O) = (Ba(OH)_2) \quad , \qquad (4)$$

and become the dominant alkaline-earth vapor species. Figure 3 shows the equilibrium pressure of $Ba(OH)_2$ due to reaction (4) for steam pressures of 1, 10, and 100 bar and for a range of temperatures from 1000 to 3000 K. Also included in Fig. 3 (as the dashed line) is the vapor pressure of $Ba(OH)_2$ over the liquid form, which fixes the upper value of $Ba(OH)_2$ partial pressure for each temperature. That is, whenever equilibrium

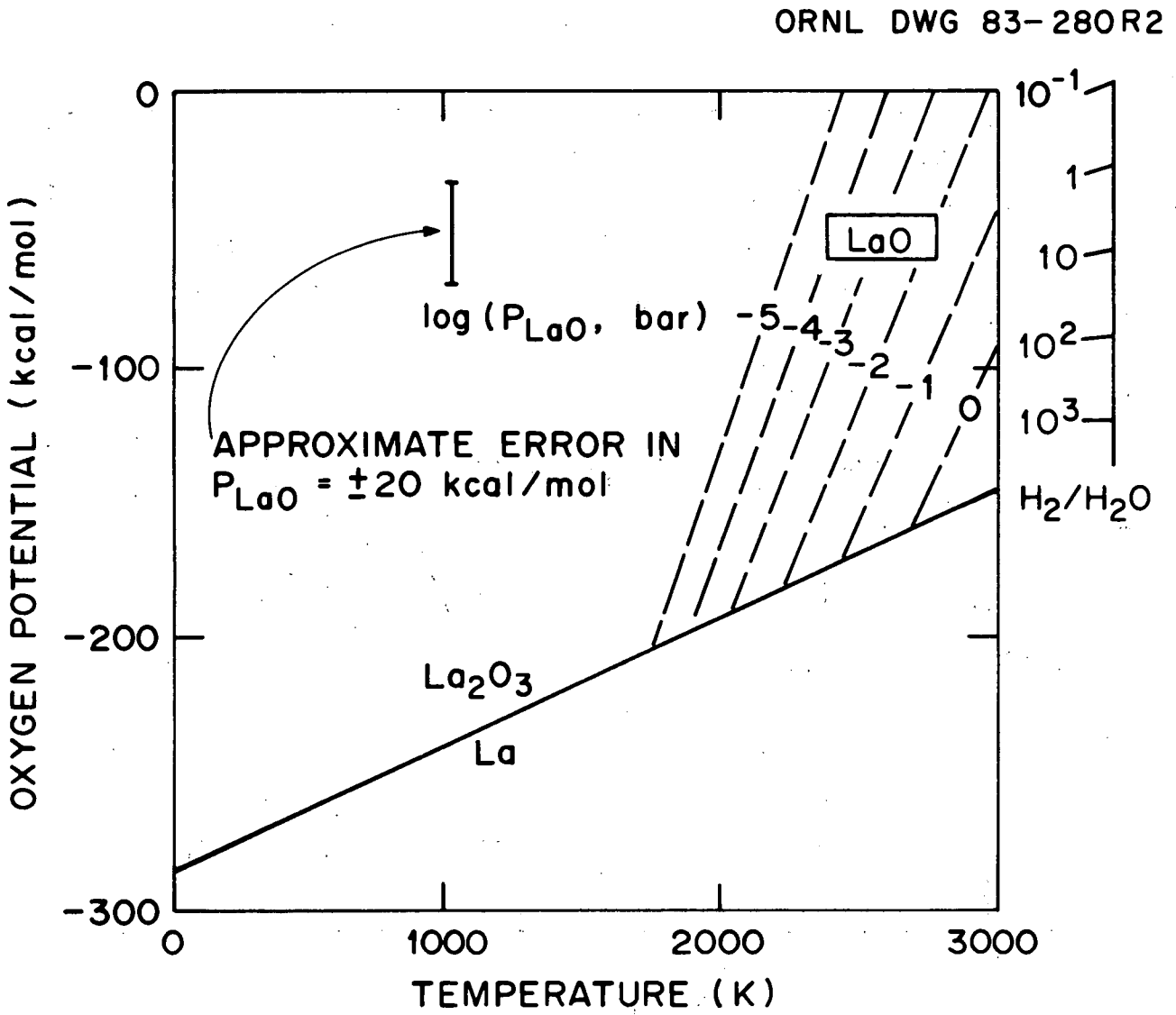

Fig. 1. Volatility of lanthanum oxide due to the reaction $2\langle La_2O_3\rangle = 4(LaO) + (O_2)$.

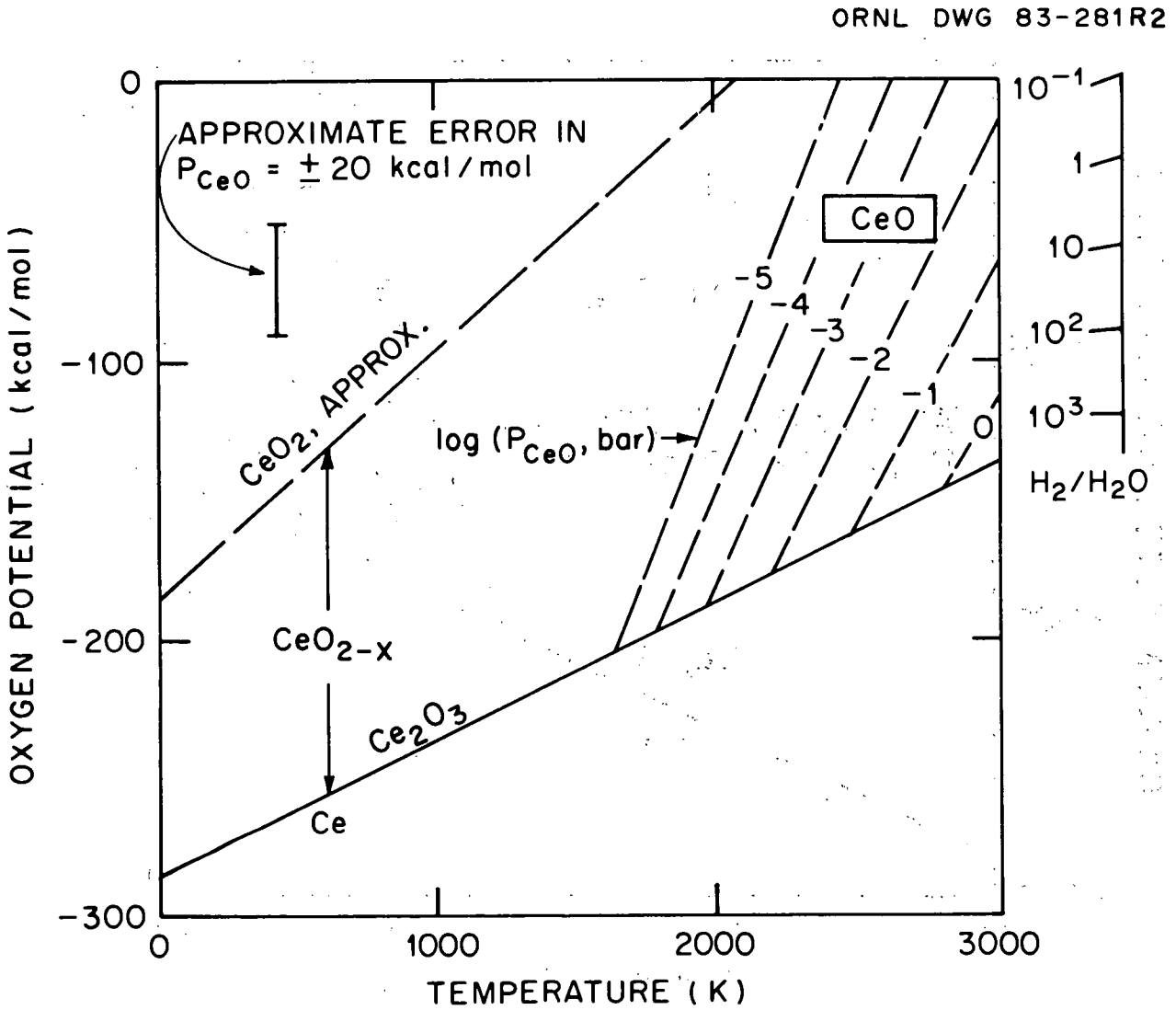

Fig. 2. Volatility of cerium oxide due to the reaction $2\langle Ce_2O_3\rangle = 4(CeO) + (O_2)$.

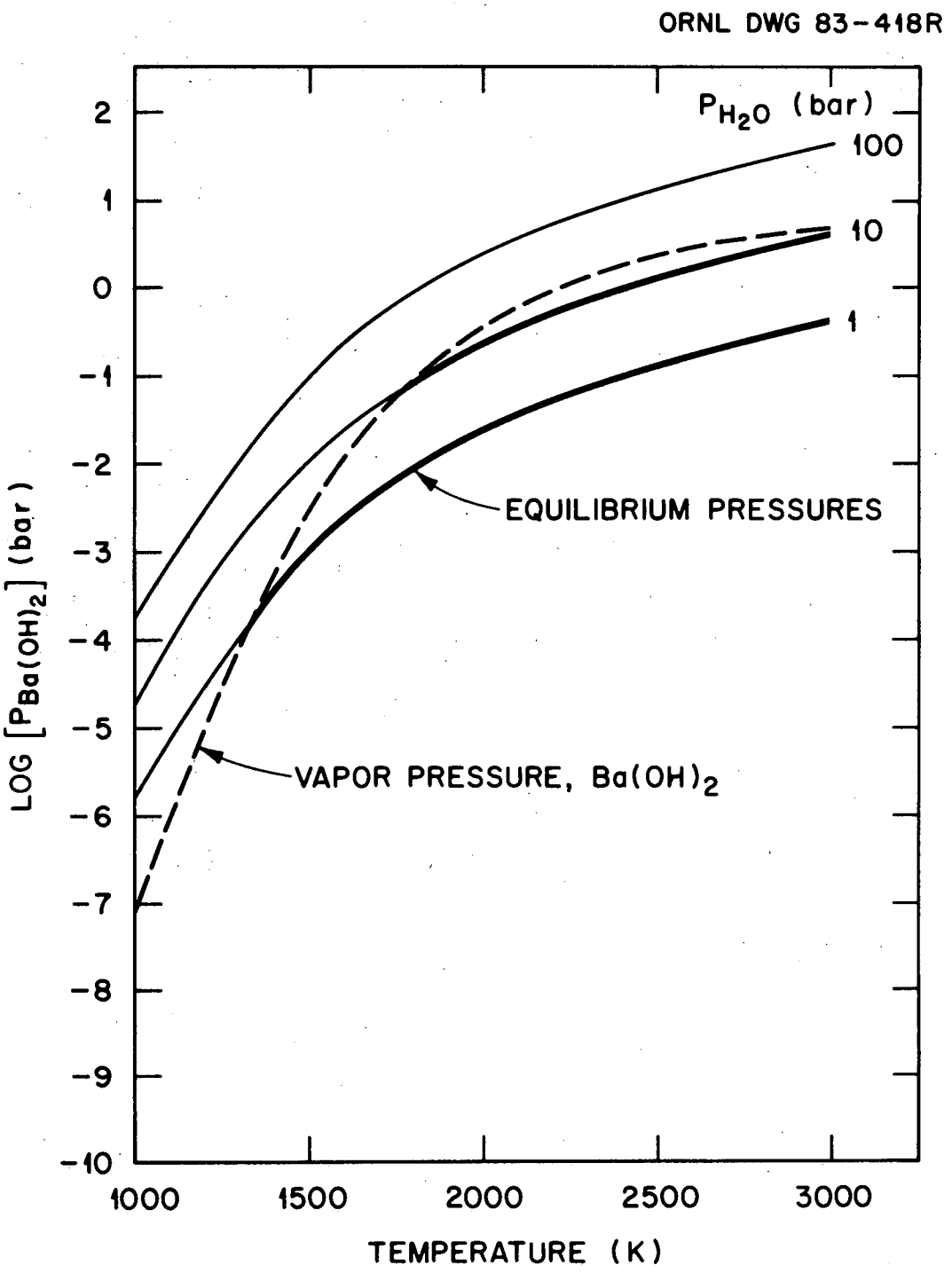

Fig. 3. Equilibrium pressure of $Ba(OH)_2$ from the reaction $\langle BaO \rangle + (H_2O) = (Ba(OH)_2)$ and vapor pressure of $Ba(OH)_2$ above the liquid.

pressures [via reaction (4)] in excess of the vapor pressure are predicted, liquid $Ba(OH)_2$ would be expected to condense until the partial pressure becomes equal to the vapor pressure at the given temperature.

From Fig. 3, we see that the maximum partial pressure of $Ba(OH)_2$ up to ~1280 K is fixed by its vapor pressure. Equilibrium pressures of the hydroxide less than the vapor pressure may be possible above ~1250 K, provided steam pressures are below ~10 bar. Thus, at temperatures above ~1250 K, the partial pressure of $Ba(OH)_2$ would also depend on the steam partial pressure.

Although BaO and $Ba(OH)_2$ were used here for illustration in the above discussion, the comments would apply fairly closely to the SrO/ $Sr(OH)_2$ system as well.

The effective vapor pressure of an alkaline-earth species may depend on the value of the steam partial pressure at low steam pressures (such as would occur in a loss-of-pressure sequence). Thus, the barium and strontium pressures would be significantly lower for temperatures above ~1250 K. Rather than take steam pressure as a variable parameter, we will assume an alkaline-earth vapor pressure corresponding to the value for the hydroxide above the liquid (i.e., by the dashed line in Fig. 3). As a result of this assumption, the estimated barium and strontium degrees of vaporization into aerosol material would represent maximal estimates; low steam pressures could result in significantly lower values. From Fig. 3, we see that the designated vapor pressure of $Ba(OH)_2$ at 2700 K is given as 3.2 bar, which is the value employed for BaO in Table 3.

3.4 DEGREE OF VAPORIZATION OF CORE MATERIAL

The effective vapor pressure of each core constituent listed in Tables 1—3 was used to determine the amount vaporized into a closed space of 548 m^3 (a typical BWR reactor vessel volume) at 2700 K. The results are listed in Table 5 for a PWR core with and without silver alloy control rods. Table 6 represents the case for a BWR core.

Table 5 shows that the silver alloy material may be expected to form a major portion of the aerosols produced from overheated PWR cores containing silver control rods. Twenty-four percent of the silver, 47% of the indium, and 100% of the cadmium in the rods are expected to vaporize and condense into aerosols, according to the assumptions used in this estimate. Of the structural materials, only manganese and chromium are projected to contribute more than ~1% to the aerosol mass. The total amount of aerosol produced is estimated to be 1282 kg, which represents ~1% of the core mass.

Table 5 also shows the estimated composition of the aerosol when the silver alloy material is omitted. The largest component of the aerosol in that case would be cesium (mainly CsOH at ~65%), with iodine (as CsI)

Table 5. Estimated vaporized fractions for PWR cores with and without silver alloy control rods

Element	Percent vaporized	Condensing form[a]	Mass vaporized (kg)	Mass of aerosol[b] (%) With control rods	Mass of aerosol[b] (%) Without control rods
		Structure			
Zr	2.6×10^{-5}	ZrO_2	0.006		
Sn	0.55	SnO_2	1.6	0.13	0.47
Fe	0.36	FeO	6.4	0.50	1.9
Cr	2.3	Cr_2O_3	12.4	1.0	3.6
Mn	28.2	MnO	14.6	1.1	4.3
Ni	0.51	Ni°	1.0	0.08	0.29
		Control rods			
Ag	24	Ag°	532	41.5	
In	47	In_2O_3	242	19.9	
Cd	100	Cd°	162	12.6	
		Fuel and fission products			
U	1.7×10^{-3}	UO_2	1.3	0.10	0.38
I, Br	100	CsI	37.9	3.0	11.0
Cs, Rb	100	CsOH	222	17.3	64.2
Te	100	Te°	32.3	2.5	9.5
Ba, Sr	2.7	$Ba(OH)_2$	5.3	0.41	1.5
Rare earths	0.06	La_2O_3	0.4	0.03	0.12
Noble metals		NM°			
Pd	3.8		3.7	0.29	1.1
Rh	2.5		0.76	0.06	0.22
Ag	100		6.3	0.49	1.8
Total (1% of core vaporized)			1282		
Less control rod materials			936		
Total without control rod (0.13% of core vaporized without control rod)			346		

[a]See Sect. 5. Superscript ° indicates elemental form.

[b]Assumed to be all the mass vaporized.

and Te° contributing 11 and ~10%, respectively. The total quantity of aerosol produced is estimated to be 346 kg, or ~0.13% of the total core mass.

Table 6 contains the calculated results for a BWR core. These results are very similar to those for the PWR case without silver control rods. The fission products, cesium, iodine, and tellurium, are the main aerosol contributors. The addition of Inconel in the structure made chromium (at 3.8%) a larger contributor to aerosol formation than manganese (at 2.2%) and increased the importance of nickel to 1.2%. The total amount for BWRs is estimated to be 660 kg, or 0.2% of the total core mass.

Table 6. Estimated vaporized fractions for BWR cores

Element	Percent vaporized	Condensing form[a]	Mass vaporized (kg)	Mass of aerosol[b] (%)
		Structure		
Zr	7.2×10^{-6}	ZrO_2	0.006	
Sn	0.15	SnO_2	1.7	0.26
Fe	0.053	FeO	6.4	0.99
Cr	0.16	Cr_2O_3	24.8	3.8
Mn	3.0	MnO	14.8	2.2
Ni	0.047	Ni°	7.7	1.2
Al	0.54	Al_2O_3	1.9	0.3
		Fuel and fission products		
U	7.9×10^{-4}	UO_2	1.3	0.2
I, Br	100	CsI	80.0	12.1
Cs, Rb	100	CsOH	437	66.2
Te	100	Te°	68.0	10.3
Ba, Sr	1.3	$Ba(OH)_2$	5.3	0.8
Rare earths	0.03	La_2O_3	0.4	0.06
Noble metals (NM)		NM°		
Pd	1.8		3.7	0.56
Rh	1.2		0.76	0.12
Ag	49.0		6.4	0.97
Total (0.2% of core vaporized)			660	

[a]See Sect. 5. Superscript ° indicates elemental form.

[b]Assumed to be all the mass vaporized.

3.5 EFFECT OF BORON SOURCES ON COMPOSITION OF THE AEROSOLS

Sources of boron were not included in the phases given in Tables 1 and 2 and the subsequent calculations and analyses that gave the aerosol compositions listed in Tables 5 and 6. As will be seen, boron may add substantially to the mass vaporized in both PWRs and BWRs and change the chemical nature of the condensing species. The boron material will be considered as a separate phase from those already discussed in this report; it is quite different for the two reactor types.

Two potential sources of boron, borosilicate glass and boric acid solution, exist for PWRs. Borosilicate glass is contained in 24 burnable poison rods located in the outer periphery of the core. It is a class of glasses made from a varying mixture of the following oxides: SiO_2, B_2O_3, Na_2O, Al_2O_3, K_2O, CaO, and Li_2O. The main constituents are SiO_2 (66–81 wt %) and B_2O_3 (13–28 wt %). The Sandia report gives the borosilicate glass composition as 82.2 kg (181 lb) of boron and 138 kg (303 lb) of silicates.[4] The 82.2 kg (181 lb) of boron is equivalent to 265 kg (583 lb) of B_2O_3. Assuming that the boron in the PWR glass is B_2O_3 and the silicates are SiO_2, this glass consists of 65.8 wt % B_2O_3 and 34.2 wt % SiO_2, a composition obviously far different from that of the typical borosilicate glass. A eutectic containing only 2.6 wt % SiO_2 melts at ~450°C (lower than the 460°C melting point of B_2O_3) to give a mixture of solid quartz and liquid B_2O_3-SiO_2. The SiO_2 content of the liquid increases until the melting point (~660°C) is reached for this particular composition (65.8% B_2O_3–34.2% SiO_2). We shall consider this glass as a single phase of B_2O_3 and SiO_2, and we will evaluate it for the effective vapor pressures of the two components at 2700 K.

The quantity of boric acid in PWRs is quite variable, depending on the core life and the quantity of coolant in the reactor. Immediately following a fresh core load, the coolant contains enough boric acid [1.25 g/L (1250 ppm)] to keep the reactor from going critical when the control rods are withdrawn. Even after the concentration is decreased to allow criticality, a fairly high boric acid content is maintained throughout most of the core life, although it is gradually decreased. Just prior to a reload, the concentration is reduced to zero to help burn off fission products and transuranics. In the previous sections of this report, the assumption was made that 548 m^3 of gas space existed in the reactor vessel, which is essentially all the void volume available in a BWR pressure vessel. In other words, no liquid coolant is present. If the accident begins with a complete loss of coolant, this assumption is valid; however, no boric acid will be present in the core. If the core overheating occurs with some or all of the coolant remaining, to end with only gas space requires that we postulate either loss of integrity in the primary system that allows boiloff of the coolant (which will decompose the boric acid to B_2O_3) or very high pressures in the pressure vessel (which will also produce B_2O_3 from the trapped boric acid). For the purposes of this report, let us assume that 0.5 g/L (500 ppm) of boric acid (approximate average over core life) and 548 m^3 of liquid coolant are trapped in the pressure vessel. In this case, 154 kg of B_2O_3 vapor would be present in the pressure vessel from the trapped boric acid. Table 7 summarizes the

Table 7. Amounts and properties of boron sources in a PWR core

Constituent	Amount (kg)	Amount (mol)	Mol fraction in phase[a]	Evaporating material: Form	Evaporating material: Melting point (°C)	Evaporating material: Boiling point (°C)	Temperature = 2700 K (1417°C): Vapor pressure (bar)	Temperature = 2700 K (1417°C): Effective vapor pressure[b] (bar)	Temperature = 2700 K (1417°C): Maximum pressure[c] (bar)
				Borosilicate glass					
B	82.2	7.60×10^3	0.62	B_2O_3	460	1860	14.4	9.0	1.5
Si	64.4	2.29×10^3	0.38	SiO_2	1713[d]	2230	2.1	0.79	0.93
				Boric acid					
B	47.8	4.42×10^3	1.0	B_2O_3	460	1860	14.4	14.4	0.90

[a]Assumed phases: B_2O_3-SiO_2 and B_2O_3.

[b]Assuming that Raoult's law applies for each phase.

[c]Pressure if material is completely vaporized at 2700 K in a 548-m^3 volume.

[d]For crystobalite. Melting point for quartz is 1610°C. Boiling point is the same for different forms.

amounts of boron available in the PWR based on the above assumptions. Boric acid decomposes at 300°C according to the following stoichiometric expression:

$$2H_3BO_3 \rightarrow 3H_2O + B_2O_3 \ .$$

Since the critical temperature of H_2O is 374°C, we have assumed that the boric acid becomes anhydrous B_2O_3 and composes a separate phase of its own.

Two potential sources of boron also exist for BWRs: B_4C control rods, and a sodium pentaborate solution to be injected in the event of a failure to scram. The Sandia reference indicates that 530 kg (1168 lb) of boron are contained in the control rods of a BWR core;[4] however, Beahm[9] has acquired more recent information indicating that 793 kg (1746 lb) of boron are in the control rods. For the purposes of this report, we will use the latter figure (793 kg). Although the B_4C does not have a significant vapor pressure at 2700 K (melting point, 2623 K), it can contribute significantly to the vapor cloud by reacting with steam to give B_2O_3, CO, CO_2, and CH_4; the ratio of products will depend on the H_2/H_2O ratio in the reactor vessel.[9] Thus, the B_4C control rods can react with the steam to produce significant quantities of CO, CO_2, and/or CH_4. Most importantly, the final form of the boron at 2700 K is B_2O_3.

Boiling-water reactors have 17,000 L (4500 gal) of 13.4 wt % $Na_2B_{10}O_{16}\cdot 10H_2O$ in reserve in case the reactor should fail to scram. In such an event, this solution would be injected at the rate of 212 L/min (56 gpm) into the core and would keep the core noncritical with a full reactor vessel of 0.6 g/L (600 ppm) of the borate solution. Assuming that the reactor has a volume of 548 m^3 and contains 0.6 g/L (600 ppm) of the borate, 5570 mol of boron will be present. Just as for boric acid in a PWR, one must assume boiloff of the H_2O. Borate, then, would be left in the pressure vessel, providing a source for boron to enter into aerosol formation. We have also assumed that sodium pentaborate decomposes to give B_2O_3 at 2700 K in Table 8.

Addition of B_2O_3 to the vapor compositions given in Tables 5 and 6 changes the chemical form of the important fission product species, cesium and iodine. Both CsOH and CsI react with B_2O_3 to give cesium borate;[9] therefore, the caustic, reactive CsOH in Tables 5 and 6 will be replaced by cesium borate and the iodine will be released from CsI, perhaps as I_2 or HI. Enough boron is present in the borosilicate glass of PWRs and the B_4C control rods of BWRs to tie up all the cesium in the fuel and yet have free B_2O_3. Of course, there are still serious questions concerning the availability of the boron for these reactions in a real reactor accident.

For the PWR case, the glass rods are located on the outer periphery (which may survive), while the center of the core undergoes meltdown and no boron may be contributed from the coolant. For the BWR case, the stainless steel tubes holding the B_4C control rods will fail at 1400 to 1500°C, exposing the B_4C to the steam environment; thermodynamically,

Table 8. Amounts and properties of boron sources in a BWR core

Constituent	Amount (kg)	Amount (mol)	Mol fraction in phase[a]	Evaporating material: Form	Evaporating material: Melting point (°C)	Evaporating material: Boiling point (°C)	Temperature = 2700 K (1417°C): Vapor pressure (bar)	Temperature = 2700 K (1417°C): Effective vapor pressure[b] (bar)	Temperature = 2700 K (1417°C): Maximum pressure[c] (bar)
				B_4C control rods					
B	793	7.34×10^4	1.0	B_2O_3	460	1860	14.4	14.4	14.8
				Borate solution					
B	60.2	5.57×10^3	0.71	B_2O_3	460	1860	14.4	10.2	1.1
Na	25.6	1.11×10^3	0.29	NaOH	318	1390	58.0	17.0	0.45

[a]Assumed phases: B_2O_3 and B_2O_3-NaOH.

[b]Assuming that Raoult's law applies for each phase.

[c]Pressure if material is completely vaporized at 2700 K in a 548-m^3 volume.

however, the B_4C will react completely as long as steam is available. The kinetics of this interaction are unknown. In fact, the reaction of steam with B_4C rods may be severely limited by mass transfer or by the chemical reaction rate. Furthermore, if the B_4C contribution is used, the borate solution should not be used since the reactor has obviously scrammed. If the reactor fails to scram, the borate solution will be used and the B_4C rods are still available below the reactor in case a catastrophic melt-through occurs. The most likely course (and the one that gives maximum availability of boron) in the BWR is that the B_4C rods will remain in place to damp criticality and the borate solution will never be used.

The large amounts of B_2O_3 that are vaporized and their effect on the chemical composition of the vapor cloud (and the resulting aerosol cloud) mean that boron cannot be ignored, but the uncertainties over kinetics and mass transfer mean that the case without boron is also important. For this reason, Tables 5 and 6 were developed without considering any contribution from boron. Tables 9 and 10 were developed to give the quantities vaporized (and aerosol composition), assuming that the boron sources were completely reacted and at equilibrium at 2700 K in a volume of 548 m^3. Table 7 was combined with data from Table 5 to obtain Table 9 for PWRs. Similarly, Table 8 was combined with Table 6 to obtain Table 10 for BWRs.

In summary, if the borosilicate glass in PWRs becomes available, the cesium released from the fuel will be tied up as a borate or silicate, which would be limited only by mass transfer. Potentially, enough boron is present to contribute 15.8% as $CsBO_2$ in the resulting aerosol while still contributing 20% as B_2O_3; silica can contribute 6.5%. The silver alloy control rods are still major aerosol contributors; however, if these control rods are not considered, boron becomes even more important in the aerosol cloud. The relative importance of the refractory materials from the structure does not change by including boron since B_2O_3 melts at a low temperature and is not a refractory material in the same sense as the other structural materials. Thus, the most abundant refractory materials in the PWR aerosol cloud are still (in decreasing order): (1) manganese oxide, (2) chromium oxide, and (3) iron or iron oxide.

If the B_4C control rods of BWRs are readily available to the steam atmosphere and react quickly, 75.1% of the resulting aerosol will be B_2O_3 with cesium trapped as $CsBO_2$ to account for an additional 18.9% contribution. Thus, boron dominates the aerosol cloud for BWRs. As for PWRs, the relative importance of the structural materials in the BWR aerosol cloud remains unchanged (in decreasing abundance): (1) chromium oxide, (2) manganese oxide, (3) nickel, and (4) iron or iron oxide.

3.6 COMPARISON WITH OTHER ESTIMATES

A few estimates of the degree of aerosol formation in the core following a loss-of-cooling event are now available, and perhaps it will be useful to compare our predictions with these. We will limit our comparison to the so-called structural aerosols, consisting of steel and

Table 9. Estimated vaporized fractions for PWR cores with and without silver alloy control rods containing boron

Element	Percent vaporized	Condensing form	Mass vaporized (kg)	Mass of aerosols (%)[a] With control rods	Mass of aerosols (%)[a] Without control rods
		Structure			
Zr	2.6×10^{-5}	ZrO_2	0.006		
Sn	0.55	SnO_2	1.6	0.09	0.18
Fe	0.36	FeO	6.4	0.35	0.74
Cr	2.3	Cr_2O_3	12.4	0.69	1.4
Mn	28.2	MnO	14.6	0.81	1.7
Ni	0.51	Ni°	1.0	0.061	0.11
		Control rods			
Ag	24	Ag°	532	29.5	
In	47	In_2O_3	242	13.4	
Cd	100	Cd°	162	9.0	
		Burnable poison			
B	100	B_2O_3	362	20.0	41.6
Si	85	SiO_2	117	6.5	13.4
		Fuel and fission products			
U	1.7×10^{-3}	UO_2	1.3	0.07	0.15
I, Br	100	I_2	18.5	1.0	2.1
Cs, Rb	100	$CsBO_2$	286	15.8	32.9
Te	100	Te°	32.3	1.8	3.7
Ba, Sr	2.7	$Ba(OH)_2$	5.3	0.29	0.61
Rare earths	0.06	La_2O_3	0.4	0.02	0.05
Noble metals		NM°			
Pd	3.8		3.7	0.20	0.43
Rh	2.5		0.76	0.04	0.09
Ag	100		6.3	0.35	0.72
Total (1.4% of core vaporized)			1806		
Less control rod materials			936		
Total without control rod (0.33% of core vaporized without control rod)			870		

[a]Assumed to be all the mass vaporized.

Table 10. Estimated vaporized fractions for BWR cores containing boron

Element	Percent vaporized	Condensing form	Mass vaporized (kg)	Mass of aerosols (%)
		Structure		
Zr	7.2×10^{-6}	ZrO_2	0.006	
Sn	0.15	SnO_2	1.7	0.06
Fe	0.053	FeO	6.4	0.21
Cr	0.16	Cr_2O_3	24.8	0.82
Mn	3.0	MnO	14.8	0.49
Ni	0.047	Ni°	7.7	0.26
Al	0.54	Al_2O_3	1.9	0.06
		Control rods		
B	97	B_2O_3	2258	75.1
		Fuel and fission products		
U	7.9×10^{-3}	UO_2	1.3	0.04
I, Br	100	I_2	39.1	1.3
Cs, Rb	100	$CsBO_2$	567	18.9
Te	100	Te°	68.0	2.3
Ba, Sr	1.3	$Ba(OH)_2$	5.3	0.18
Rare earths	0.03	La_2O_3	0.4	0.01
Noble metals		NM°		
Pd	1.8		3.7	0.12
Rh	1.2		0.76	0.03
Ag	49.0		6.4	0.21
Total (1.9% of core vaporized)			3007	

Inconel plus cladding material. These materials, which have the lowest volatilities, would condense first on departure from the core region. As such, they would very likely provide a gas-borne surface for condensation of the more volatile materials (e.g., semivolatile fission product species and metallic control rod materials), which would provide the major portion of the aerosol mass in temperature regions that permit their condensation.

The degree to which the higher-volatility materials would add to the aerosol mass in cooler regions of the reactor vessel simply by condensing onto adjacent structural surfaces needs to be determined. This relative rate will depend on the relative driving force for condensation onto

solid surfaces (which are usually cooler) compared with the driving force for condensation onto the existing aerosol particles (which assume the normally hotter gas temperature). In addition, mass transfer differences for aerosol condensation onto these two types of surfaces need to be taken into account in the determination of the relative competition for condensation between solid structural and gas-borne aerosol surfaces.

Table 11 lists five recent estimates of the amounts of aerosol that would be produced by the condensation of structural materials. Note that the equilibrium thermodynamic estimate developed by the relatively simple procedure adopted in the present study appears to be in fair agreement with two other recent estimates. Our estimates (taken from Tables 5 and 6) indicate that 36 to 57 kg of structural aerosol will be produced, compared with <17 kg predicted by a model developed by Lorenz[10] employed in current work.[2,11] In addition, they appear to be consistent with those being developed in Core-Melt Studies work,[12] wherein a portion (<1 kg) of representative core materials is heated to the melting point of the mixture. Linear extrapolation of such results to the size of a PWR core indicates that ~11 kg of structural materials would form aerosol material.

As noted in Table 11, the predicted degree of structural aerosol formation based on test data obtained in the German SASCHA program[13] is significantly higher than the above estimates. No clear reason for this divergence is currently known. It is not surprising, however, that the NUREG-0772 estimates[1] agree with the SASCHA test results since the SASCHA data were used in the NUREG-0772 calculations.

4. OXYGEN POTENTIALS IN THE REACTOR VESSEL

The chemical forms of the various metallic vapors condensing into aerosols in the reactor vessel depend primarily on the oxygen potential existing in the gas space. The principal constituents of the gas are steam and hydrogen generated from the reaction of water and zirconium, and the oxygen potential depends on the relative amounts of these two gases.

The estimated ratio of hydrogen to steam (H_2/H_2O) in the reactor vessel as a function of time from initial cladding failure is illustrated in Fig. 4 for two cases.[2,11] Note that while these results were generated by a current version of the MARCH program,[14] both cases appear to indicate that the H_2/H_2O ratio increases with time from initially low values (~0.1 at the time of initial fuel melt) to ~1–10 at later times. The increase in the ratio with time appears to be reasonable in view of the projected increase in hydrogen generation rate as the average temperature rises. Thus, reactor vessel conditions may be expected to become progressively more reducing with time, provided that the two cases examined are actually typical. Based on the results of these two cases, the ratio values from initial fuel melt to reactor vessel failure appear to range from ~0.1 to 10.

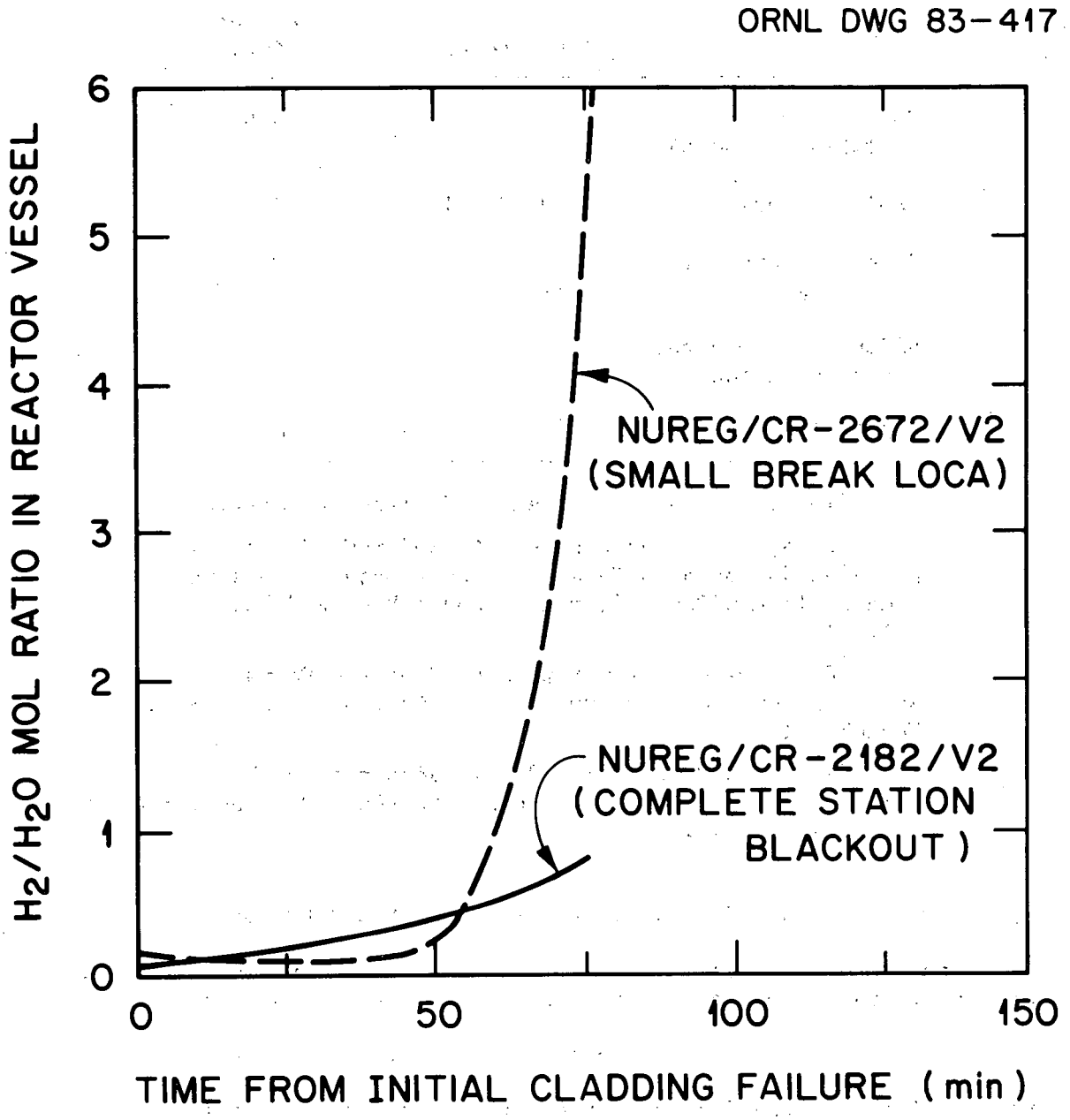

Fig. 4. Estimated H_2/H_2O ratios in the reactor vessel from time of initial cladding failure.

Table 11. Predicted amounts of structural aerosol[a] formed under core-melt conditions

Source	Reference	Amount (kg)
This study (Tables 5 and 6)		36–57
SASA estimate[b]	10, 2, 11	~17
Parker — Core melt studies[c]	12	10.7
SASCHA data — direct extrapolation	15	738
NUREG-0772[d]	1	~250

[a]Includes steel, Inconel, and cladding materials.

[b]Based on Lorenz's model [NUREG/CR-0027, vol. 1, pp. 1090-99] used in Severe Accident Sequence Analysis studies [NUREG/CR-2182, vol. 2 and NUREG/CR-2672, vol. 2].

[c]G. W. Parker, paper presented at the German/American Core-Melt Information Meeting, Karlsruhe, FRG, November 1982.

[d]Appendix B, NUREG-0772; excludes mass of bottom structure. If this is included, the NUREG-0772 estimate would be ~700 kg.

5. CHEMICAL FORMS OF REACTOR VESSEL AEROSOLS

Whether aerosol materials exist in the oxidic or the reduced form depends primarily on the oxygen potential; that is, the reaction,

$$\langle MO_2 \rangle = \langle M \rangle + (O_2) \ ,$$

with equilibrium coefficient defined to a first approximation as

$$K = P_{O_2} \ ,$$

will be driven to the left for cases when the oxygen partial pressure is maintained above K.

Two conditions must exist for this approximation to hold. First, both the oxide and the reduced form must have sufficiently low volatility

to allow the existence of the condensed phase. When this is not the case, a reaction with simple equilibrium constant depending only on the oxygen pressure cannot be written. A second requirement is that the activity of the condensed phase be ~1, as would normally be the case when it exists in a relatively pure form. However, this would not be a good assumption for low concentrations of materials in solution where both the concentration and the activity coefficient need to be taken into account in the definition of the equilibrium constant.

Figure 5 illustrates the oxide-to-reduced form transition as a function of temperature for a number of possible structural aerosols. In each instance, oxygen potentials above the indicated transition line would indicate that the oxidized form is predicted to exist. The shaded region indicates the approximate range of oxygen potentials that may be expected in a reactor vessel during the course of an accident. These potentials correspond to H_2/H_2O ratios ranging from ~0.1 to ~10, as shown on the scale at right. As mentioned in the previous section, the oxygen potential appears to be a function of time, with the values being generally higher (lower H_2/H_2O ratios) in the early part of the event and then declining to a much lower level later in the sequence due to continued hydrogen production.

Figure 5 shows that some elements are clearly metallic and others clearly oxidic for the given range of oxygen potentials. The transitions for Ni, Cd, Ag, Rh, Pd, and Ru are far above any possible oxygen potential that may exist; hence these elements would exist as metals. Conversely, the transition lines for Zr, Al, rare earths, U, Ba, Sr, Cr, Mn, Nb, and Si fall below the expected range of oxygen potentials and thus would be expected to be oxidic.

Figure 5 also shows that a number of important aerosol constituents may be in either the reduced or the oxidic form, depending on the local or current values for temperature and H_2/H_2O ratio. Most significantly, the FeO/Fe, MoO_2/Mo, and In_2O_3/In transitions fall within the possible range of oxygen potentials for all temperatures. Therefore, these elements may exist in either form, depending on local conditions, or may perhaps change with time during the event. If this change does occur, the earlier form will probably be the oxide, which will be converted to the reduced form with increased levels of H_2.

Figure 5 shows that tin would likely exist as the metal except early in the event when H_2/H_2O >~1 and for the cooler locations (temperature, <~600°C). Interestingly, the CdO/Cd system does not appear to conform to the original assumption of low volatility for condensed forms (the boiling point for cadmium is only 765°C). However, as noted in Table 5, the mass of cadmium in the primary system creates sufficiently high cadmium metal pressures to ensure formation of a condensed phase.

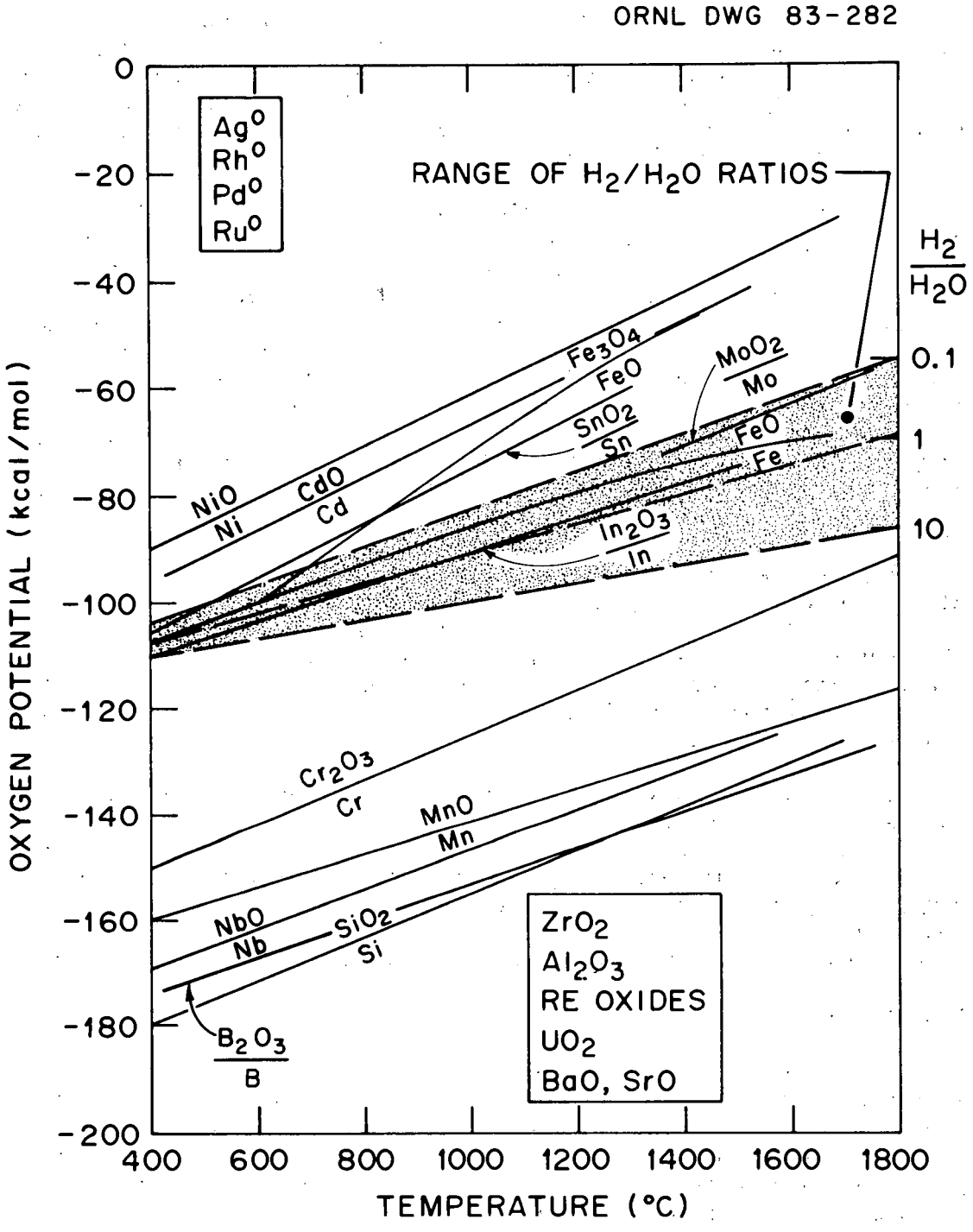

Fig. 5. Chemical forms of structural aerosols.

6. SUMMARY AND CONCLUSIONS

From the results of our study, we can draw the following conclusions:

1. Under the idealized assumptions used here (based on estimated volatilities of materials in phases assumed to be present), we estimate that ~1% of a core containing silver control rods will vaporize and condense into aerosols under LWR core-melt conditions. Approximately 1.4% of such a core vaporizes if boron is included in the calculations.

2. The major part of the aerosol mass produced in PWRs containing silver control rods is expected to be composed of elements in the silver alloy — silver, cadmium, and indium. About 74% of the aerosol is composed of these three materials when idealized assumptions are used. About 42% of the aerosol mass is silver, which is ~24% of the core inventory of that element. Boron, if included, is another large mass contributor with the control rods accounting for ~52% and boron and cesium ~36%.

3. Under the conditions of our study, ~24% of the silver inventory contained in the control rods would vaporize and subsequently condense into aerosols. This value is somewhat higher than that (i.e., 4%) measured in recent core-melt tests.[12] However, the measured value probably represents some sequestering of silver by silver-zirconium alloy formation, which was not accounted for in the present estimate.

4. In cores without silver control rods, ~0.1% of the core mass for PWRs and ~0.2% for BWRs were estimated to vaporize and subsequently condense into aerosols. Including boron changes these figures to ~0.3% and ~0.9% respectively.

5. Despite the highly idealized assumptions used here, the predicted degree of core vaporization falls within the range of estimates used in other recent studies (see Table 11).

6. In cores without silver control rods, the major aerosol components are the condensable fission product species cesium hydroxide and cesium iodide, which comprise ~76 to 79% of the total aerosol mass. Including boron changes the cesium species to cesium borate, releasing the iodine. Thus, ~42% of the aerosol mass is B_2O_3 while ~33% is $CsBO_2$.

7. The projected amounts of structural material (Fe, Zr, Sn, Mo, Cr, and Ni) vaporized and condensed into aerosol are quite low — 36 kg for PWRs and 57 kg for BWRs. Although these estimates are lower than earlier data had indicated, they are in general agreement with more recent estimates.

8. It is very important to identify the phases formed under core-melt conditions since this is the necessary first step in calculating vaporization rates. The most significant effect of alloy or solid-solution formation would be vapor-pressure reduction of the more-volatile metals.

9. Blind application of Raoult's law to dilute components of phases can lead to errors of as much as +2 to -5 orders of magnitude in estimated volatility. Activity coefficient measurements for a few critical alloy systems (e.g., Ag-Zr) would be extremely helpful for this purpose, as well as for phase identification.

10. The rare-earth oxides generate surprisingly high vapor pressures with the oxygen potentials and the temperatures that exist within irradiated UO_2. The effective volatility is generated by the typical decomposition reaction

$$\langle La_2O_3 \rangle = 2(LaO) + 1/2\ O_2\ ,$$

where the monoxide is the dominant vapor species at these temperatures. At an oxygen potential of ~ -100 kcal/mol (-418 kJ/mol, which is typical for UO_2), both the La_2O_3 and the CeO_{2-x} solid solutions exert a vapor pressure of ~0.06 bar above the pure material at 2700 K. Since rare-earth oxides are presumably in solution within the UO_2 phase, the exerted vapor pressure would be significantly reduced by dilution; however, these vapor pressures are surprisingly high for a refractory material. The question then arises as to whether high rare-earth oxide volatility might contribute to the unexpectedly high lanthanum releases observed in the Power Burst Facility (PBF) tests.[16]

11. Although there may be some internal inconsistency in the MARCH[14] program with respect to determination of the gas composition above the overheated core, it appears that the H_2/H_2O ratio in the pressure vessel increases from ~0.1 to perhaps 0.8 from the time of cladding failure to vessel melt-through. In accidents with low steam production, this ratio may briefly reach values as high as ~10.

12. The chemical forms taken by aerosol materials under the conditions existing in the pressure vessel are summarized in Table 12. The systems Fe/FeO, Sn/SnO_2, Mo/MoO_2, and In/In_2O_3 have transitions close to the predicted H_2/H_2O ratios. Other materials are either clearly metallic or clearly oxidic in this environment.

Table 12. Chemical forms of aerosols in pressure vessel prior to failure

Oxidic	Metallic	Indefinite[a]
ZrO_2	Ag	$Fe/FeO/Fe_3O_4$
Al_2O_3	Te	Sn/SnO_2
RE_2O_3	Ni	In/In_2O_3
UO_2	Cd	Mo/MoO_2
BaO	Rh	
SrO	Pd	
B_2O_3	Ru	

[a]Could be either oxidic or metallic.

7. REFERENCES

1. Technical Bases for Estimating Fission Product Behavior During LWR Accidents, Appendix C, pp. C.1-C.26, NUREG-0772, June 1981.

2. R. P. Wichner, A. D. Mitchell, R. A. Lorenz, W. J. Armento, C. F. Weber, and S. A. Hodge, Station Blackout at Browns Ferry Unit One: Iodine and Noble Gas Distribution and Release, NUREG/CR-2182, vol. 2 (ORNL/NUREG/TM-455/V2), August 1982.

3. R. Hultgren et al., Selected Values of the Thermodynamic Properties of Binary Alloys, American Society of Metals, Metals Park, Ohio, 1973.

4. Core Meltdown Experimental Review, SAND74-0382, 1975.

5. T. M. Besmann and T. B. Lindemer, "Chemical Thermodynamics of Cs-U-Zr-O-H-I in LWR Fuel Cladding Gap," Nucl. Technol. 40, 297 (1978).

6. T. B. Lindemer, T. M. Besmann, and C. E. Johnson, "Thermodynamic Review and Calculations — Alkali-Metal Oxide Systems with Nuclear Fuels, Fission Products, and Structural Materials," J. Nucl. Mater. 100(1-3), 178-226 (1981).

7. R. L. Pearson and T. B. Lindemer, Simulated Fission Product Oxide Behavior in Triso-Coated HTGR Fuel, ORNL/TM-6741, August 1979.

8. T. B. Lindemer, ORNL, letter to R. P. Wichner, ORNL, "Calculations of Lanthanide Species Gas Pressures Under Reactor Core Meltdown Conditions," Feb. 16, 1982.

9. E. C. Beahm, personal communication, October 1983.

10. R. A. Lorenz, The Vaporization of Structural Materials in Severe Accidents, NUREG/CP-0027, vol. 1, pp. 1090-99, February 1983.

11. R. P. Wichner, C. F. Weber, A. L. Wright, S. A. Hodge, R. A. Lorenz, and J. W. Nehls, SBLOCA Outside Containment at Browns Ferry Unit One: Iodine, Cesium, and Noble Gas Distribution and Release, NUREG/CR-2672, vol. 2 (ORNL/NUREG/TM-8119/V2), September 1983.

12. G. W. Parker, "Fission Product Release and Aerosol Production on the Core-Melt Tests," presented at the German/American Core-Melt Information Meeting, Karlsruhe, FRG, November 1982.

13. D. Perinic, H. Knauss, and B. Stuka, Development and Operation of Facilities for Studying Fission Product Releases in LWR Core Meltdowns, KFK-2750, pp. 4300-36–4300-45, October 1979.

14. W. T. Pratt et al., MARCH1B: BNL Modifications to the MARCH Computer Code, NUREG/CP-0027, vol. 2, pp. 1167-76, February 1983.

15. H. Albrecht, "Fission Product Release Program at the SASCHA Facility," BMFT/USNRC Core-Melt Information Exchange Meeting, Oct. 27-8, 1982.

16. D. J. Osetek, J. J. King, and R. M. Kumar, "Fission Product Source Terms Measured During Fuel Damage Tests in the Power Burst Facility," Proceedings of the International Meeting on Thermal Nuclear Reactor Safety, Chicago, Ill., Aug. 29—Sept. 2, 1982, NUREG/CP-0027, vol. 1, p. 162, February 1983.

NUREG/CR-3181
ORNL/TM-8683
Dist. Category R3

INTERNAL DISTRIBUTION

1. R. E. Adams
2. C. W. Alexander
3. T. M. Besmann
4. D. O. Campbell
5. J. L. Collins
6. F. F. Dyer
7. G. F. Flanagan
8. J. R. Hightower
9. S. A. Hodge
10. J. K. Johnson
11. T. S. Kress
12. T. B. Lindemer
13. R. A. Lorenz
14. A. P. Malinauskas
15. K. S. Norwood
16. M. F. Osborne
17. B. R. Rogers
18. F. M. Scheitlin
19-23. R. D. Spence
24. M. G. Stewart
25. S. K. Whatley
26-31. R. P. Wichner
32. R. G. Wymer
33. Central Research Library
34. Document Reference Section
35-36. Laboratory Records
37. Laboratory Records, RC
38. ORNL Patent Section

EXTERNAL DISTRIBUTION

39. Office of Assistant Manager, Energy Research and Development, DOE-ORO, P.O. Box E, Oak Ridge, TN 37831
40-41. Director, Division of Reactor Safety Research, U.S. Nuclear Regulatory Commission, Washington, DC 20555
42-43. Technical Information Center, DOE, Oak Ridge, TN 37831
44. L. K. Chan, U.S. Nuclear Regulatory Commission, 7915 Eastern Ave., Mail Stop 1130 S.S., Silver Spring, MD 20910
45-47. M. Jankowski, U.S. Nuclear Regulatory Commission, 7915 Eastern Ave., Mail Stop 1130 S.S., Silver Spring, MD 20910
48. M. Silberberg, U.S. Nuclear Regulatory Commission, 7915 Eastern Ave., Mial Stop 1130 S.S., Silver Spring, MD 20910
49. G. Marino, U.S. Nuclear Regulatory Commission, 7915 Eastern Ave., Mail Stop 1130 S.S., Silver Spring, MD 20910
50-324. Given distribution as shown in Category R3 (NTIS — 10)

NRC FORM 335 (11-81)

U.S. NUCLEAR REGULATORY COMMISSION

BIBLIOGRAPHIC DATA SHEET

1. REPORT NUMBER (Assigned by DDC)
NUREG/CR-3181
(ORNL/TM-8683)

4. TITLE AND SUBTITLE (Add Volume No., if appropriate)
Quantity and Nature of LWR Aerosols Produced in the Pressure Vessel During Core Heatup Accidents — A Chemical Equilibrium Estimate

2. (Leave blank)

3. RECIPIENT'S ACCESSION NO.

7. AUTHOR(S)
R. P. Wichner and R. D. Spence

5. DATE REPORT COMPLETED

MONTH	YEAR
October	1983

9. PERFORMING ORGANIZATION NAME AND MAILING ADDRESS (Include Zip Code)
Oak Ridge National Laboratory
P.O. Box X
Oak Ridge, TN 37830

DATE REPORT ISSUED

MONTH	YEAR
March	1984

6. (Leave blank)

8. (Leave blank)

12. SPONSORING ORGANIZATION NAME AND MAILING ADDRESS (Include Zip Code)
Division of Accident Evaluation
Office of Nuclear Regulatory Research
U.S. Nuclear Regulatory Commission
Washington, D.C. 20555

10. PROJECT/TASK/WORK UNIT NO.

11. FIN NO.
B0127

13. TYPE OF REPORT
NUREG/CR and ORNL/TM

PERIOD COVERED (Inclusive dates)
(NA)

15. SUPPLEMENTARY NOTES

14. (Leave blank)

16. ABSTRACT (200 words or less)

The degree of vaporization of LWR core materials was estimated using a highly idealized procedure involving (1) specification of the phases that are present for both structural and fuel material; (2) estimation of the vapor pressures exerted by the individual components of each phase; and (3) assuming a degree of vaporization of each phase constituent, to allow equilibration between gaseous and condensed species within the assumed pressure vessel volume. Obviously, the degree of vaporization of many core materials is limited by other complex factors such as local mass transport conditions and solid-phase diffusion rates; however, the results obtained in this study serve to illustrate the types of driving forces for vaporization that are present and to give some indication of the composition of the vaporized material. Some comparisons are provided with estimated degrees of core vaporization from other sources.

In addition to estimated degrees of vaporization, information is included regarding the projected chemical forms of the condensed material for the expected range of oxygen potentials in the reactor vessel.

17. KEY WORDS AND DOCUMENT ANALYSIS

17a. DESCRIPTORS

LWR accidents, aerosols, fission products, LWR source term, core-melt

17b. IDENTIFIERS/OPEN-ENDED TERMS

18. AVAILABILITY STATEMENT

19. SECURITY CLASS (This report)
Unclassified

20. SECURITY CLASS (This page)
Unclassified

21. NO. OF PAGES

22. PRICE
$